Journal of Photochemistry and Photobiology A: Chemistry 198 (2008) 144–149

Contents lists available at ScienceDirect

Journal of Photochemistry and Photobiology A: Chemistry

journal homepage: www.elsevier.com/locate/jphotochem

Effect of iron salt on the color removal of water containing the azo-dye reactive blue 69 using photo-assisted Fe(II)/H_2O_2 and Fe(III)/H_2O_2 systems

Sayra L. Orozco[a,1], Erick R. Bandala[b,2], Camilo A. Arancibia-Bulnes[a,*,1], Benito Serrano[c], Raúl Suárez-Parra[a,1], Isaias Hernández-Pérez[d]

[a] Centro de Investigación en Energía, Universidad Nacional Autónima de México, Priv. Xochicalco S/N, Temixco, Morelos 62580, Mexico
[b] Departamento de Ingenieria Civil y Ambiental, Escuela de Ciencias e Ingenieria, Universidad de Las Americas-Puebla, Sta. Catarina Martir, Cholula, 72820 Puebla, Mexico
[c] Fac. Ciencias Químicas, Universidad Autónoma de Zacatecas, Km 0.5 Carretera Cd. Cuauhtémoc, Guadalupe, 98600 Zacatecas, Mexico
[d] División de Ciencias Básicas e Ingeniería, Universidad Autónoma Metropolitana-Azcapotzalco, Av. Sn. Pablo 180, Col. Reinosa, 02200 México, DF, Mexico

ARTICLE INFO

Article history:
Received 6 December 2007
Received in revised form 3 March 2008
Accepted 4 March 2008
Available online 13 March 2008

Keywords:
Azo dye
Photo-Fenton process
Color removal
Hydrogen peroxide
Iron salt counter ion

ABSTRACT

The effect of chloride, sulfate and nitrate anions on the color removal of water containing the azo-dye reactive blue 69 (RB69) in acidic solution, by using photo-assisted Fenton process with Fe(II)/H_2O_2 and Fe(III)/H_2O_2 systems was investigated. Experiments were conducted in a batch reactor irradiated during 5 h with a domestic 15 W lamp with emission in the visible spectra. Experimental results showed color disappearance in the first 5 min of reaction in the photo-assisted process for all of the different salts, greatly enhancing the reaction rate with respect to the corresponding systems under dark conditions. The exception of the general trend was the $Fe_2(SO_4)_3$/H_2O_2/UV system, where the decolorization process is slower probably because the oxidative species generated by rupture of Fe(III)–peroxo complexes are less reactive. Total organic matter depletion and mineralization of the effluent were also tested during the experimental runs by means of total organic carbon (TOC) showing that, for most of the photo-assisted experiments high mineralization was reached after 3 h of reaction.

1. Introduction

Textile activities are highly water intensive and its effluents are usually strongly colored, containing high concentrations of dyes, tensoactive compounds, chrome, suspended solids, and high chemical oxygen demand (COD) [1]. The presence of dyestuff in textile wastewater is aesthetically offensive, inhibits photosynthetic processes in water bodies and, in many cases, generates toxicity to aquatic organisms and humans [2]. Most dyes contained in textile effluents are designed to resist oxidizing and reducing agents, washing, and light exposure. These characteristics make such chemicals highly refractory and hard to remove by using conventional wastewater treatment processes [3].

Considering discharge volume and effluent composition of wastewaters, textile industry is rated as the most polluting among all industrial sectors [4]. For this reason, water reuse in textile industry is a very interesting and environmentally desirable goal. Color is one of the most important wastewater reuse criteria for these kinds of effluents [3,5]. Complete color removal is sought if water is to be reused in fiber washing process, to avoid undesired color variations in the subsequent dyeing process.

Several emerging methodologies have been tested for the treatment of textile wastewater. Among them, Advanced Oxidation Processes (AOPs) are considered as highly efficient ones. For instance, ozonation, H_2O_2/O_3, H_2O_2/UV, O_3/UV, TiO_2/UV, and electrochemical oxidation have been tested in these effluents [3,6] with interesting results for color removal and COD depletion. Among AOPs, the photo-Fenton reaction has been shown as a very attractive, cost effective, and high efficiency process for textile wastewater decolorization, as demonstrated in several recent works [2,7–10]. For this photo-assisted process, the influence of radiation is an increase of the oxidation rates of the model pollutants, as compared to the conventional (in the dark) Fenton process. Several possible reaction schemes for photo-induced system have been proposed and the formation of different complexes studied by spectrophotometry (see Tables 1–3) [11,12,19]. From these studies, the influence of iron oxidation state and the specific counter ion of the iron salt employed have been demonstrated, both in the decomposition of H_2O_2 and in the overall efficiency of the photo-Fenton process for the oxidation of some model pollutants [12,13,17,18]. For example, Kiwi et al. [14] showed an important diminishment in the decoloration rate of Orange II by the Fe(III)/H_2O_2 system

* Corresponding author. Tel.: +52 55 56229791; fax: +52 55 56229791.
E-mail address: caab@cie.unam.mx (C.A. Arancibia-Bulnes).
[1] Tel.: +52 55 56229791; fax: +52 55 56229791.
[2] Tel.: +52 222 2292652; fax: +52 222 2290000x4199.

1010-6030/$ – see front matter © 2008 Elsevier B.V. All rights reserved.
doi:10.1016/j.jphotochem.2008.03.001

Table 1
Fenton's reactions [13,21–23]

$[Fe(II)]^{2+} + H_2O_2 \rightarrow [Fe(III)]^{3+} + HO^{\bullet} + OH^-$	(1)
$[Fe(II)]^{2+} + HO^{\bullet} \rightarrow [Fe(III)]^{3+} + OH^-$	(2)
$[Fe(III)]^{3+} + H_2O \leftrightarrow [FeOH]^{2+} + H^+$	(3)
$[Fe(III)^{3+}] + H_2O_2 \leftrightarrow [FeHO_2]^{2+} + H^+$	(4)
$[FeOH]^{2+} + H_2O_2 \leftrightarrow [Fe(OH)(HO_2)]^+ + H^+$	(5)
$[FeOH]^{2+} \rightarrow [Fe(II)] + HO^{\bullet}$	(6)
$[FeHO_2]^{2+} \rightarrow [Fe(II)] + HO_2^{\bullet}$	(7)
$[Fe(OH)(HO_2)]^+ \rightarrow [Fe(II)] + HO_2^{\bullet} + HO^-$	(8)
$RH + HO^{\bullet} \rightarrow R^{\bullet} + H_2O$	(9)

Table 2
Fenton's reaction: additional reactions by chloride anion effect [12,13,24]

$[Fe(II)]^{2+} + Cl^- \leftrightarrow FeCl^+$	(10)
$[Fe(III)]^{3+} + Cl^- \leftrightarrow FeCl^{2+}$	(11)
$[Fe(III)]^{3+} + 2Cl^- \leftrightarrow FeCl_2{}^+$	(12)
$FeCl^{2+} \rightarrow [Fe(II)]^{2+} + Cl^{\bullet}$	(13)
$FeCl_2{}^+ \rightarrow [Fe(II)]^{2+} + Cl^{\bullet}{}_2{}^-$	(14)
$[Fe(II)]^{2+} + Cl^{\bullet} \rightarrow [Fe(III)]^{3+} + Cl^-$	(15)
$[Fe(II)]^{2+} + Cl^{\bullet}{}_2 \rightarrow FeCl^{2+} + Cl^-$	(16)
$Cl^- + HO^{\bullet} \rightarrow [ClOH]^{\bullet -}$	(17)
$[ClOH]^{\bullet -} + H^+ \rightarrow [HClOH]^{\bullet}$	(18)
$[HClOH]^{\bullet} \rightarrow Cl + H_2O$	(19)
$Cl^{\bullet} + H_2O_2 \rightarrow HO^{\bullet}{}_2 + Cl^- + H^+$	(20)
$Cl^{\bullet}{}_2 + H_2O_2 \rightarrow HO^{\bullet}{}_2 + 2Cl^- + H^+$	(21)

Table 3
Fenton's reaction: additional reactions by sulfate anion [12]

$[Fe(II)]^{2+} + SO_4{}^{2-} \leftrightarrow FeSO_4$	(22)
$[Fe(III)]^{3+} + SO_4{}^{2-} \leftrightarrow FeSO_4{}^+$	(23)
$[Fe(III)]^{3+} + 2SO_4{}^{2-} \leftrightarrow Fe(SO_4)_2{}^-$	(24)
$FeSO_4{}^+ \rightarrow [Fe(II)]^{2+} + SO^{\bullet}{}_4{}^-$	(25)
$SO^{\bullet}{}_4{}^- + H_2O_2 \rightarrow SO_4{}^{2-} + HO^{\bullet}{}_2{}^- + H^+$	(26)

when using chloride salts, because of the generation of chlorinated organic products. However these works have not studied the effect of several different salts over a single model pollutant. Moreover, important amounts of anions coming from sources different than the iron salts are present in those experiments. Therefore, the effect of inorganic salts on the reaction rates is not well documented and the interpretation of experimental data is not easy because little is known about the photoreactivity of Fe(III) complexes.

The aim of this work is to further analyze the actual effect of several iron/H_2O_2 systems on the efficiency of photo-assisted Fenton reaction for water decolorization, and for organic matter depletion and mineralization. In our search to determine the best treatment condition for textile wastewater with the final goal of generating good quality reusable water, we have evaluated the influence of different iron salts on the H_2O_2 decomposition and the effect of this behavior on the photocatalyzed decolorization of water containing an azo dye.

2. Experimental

2.1. Reagents

Several Iron salts were used in the experiments as iron sources, $FeCl_2{\cdot}6H_2O$, $FeCl_3{\cdot}4H_2O$, $FeSO_4{\cdot}7H_2O$, $Fe_2(SO_4)_3{\cdot}nH_2O$, and $Fe(NO_3)_3{\cdot}9H_2O$ as well as hydrogen peroxide H_2O_2 30% stabilized. Sulfuric, chlorhydric, and nitric acids were used for pH adjustment. All of these chemicals were purchased from Fermont as A.C.S reagent grade and used as received without further purification. Reactive blue 69 (RB69), industrial grade, was supplied by CIBA.

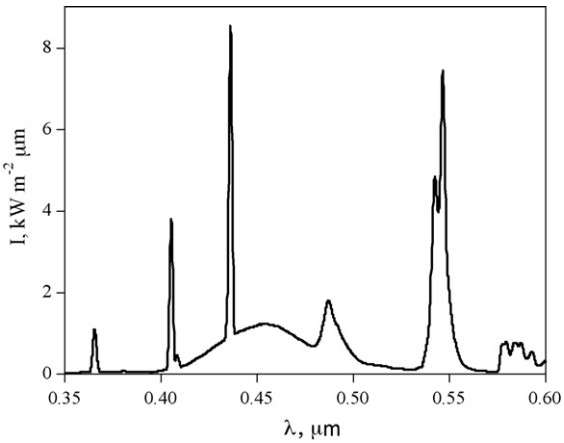

Fig. 1. Irradiation spectrum of the lamp used in this work.

2.2. Experimental procedures

Degradation of RB69 was carried out by the Fenton and photo-Fenton process, employing a batch type cylindrical reactor (500 mL total volume). The source of light is a 15 W visible light domestic lamp (Phillips).

The optical characterization for the determination of the emission from the lamp used in the experiments was carried out in a UV–Vis–IR Spectrophotometer (Shimadzu mod. UV-3101 PC). Fig. 1 depicts the actual irradiation spectrum of the lamp. It is worth to observe that the lamp emission is mostly at the visible region, with several peaks, and very low UV (3%) emission. The total radiative output of the lamp is 2.87 W.

The synthetic colored solution was prepared by dissolving 100 mg of RB69 in 1 L of water (0.14 mM). All the experiments were carried out in acidic (pH 3) conditions in order to avoid precipitation of iron oxides. The initial pH value of the solution was adjusted and kept constant by using a solution of an acid with the same anion as the iron salt employed; i.e., either sulfuric, chlorhydric, or nitric acids. The solution of the model pollutant was placed in the reactor and the transition metal catalyst (either Fe(II) or Fe(III)) was added to get a concentration of 0.13 mmol/L. The iron salts used in this study were $FeCl_2$, $FeCl_3$, $FeSO_4$, $Fe_2(SO_4)_3$, and $Fe(NO_3)_3$. The resulting anion concentrations corresponding to the above iron concentration were 0.29, 0.42, 0.15, 0.22, and 0.42 mM, respectively, for each of these salts. The reaction mixture was kept in agitation in the dark for 5 min in order to homogenize it and an initial (t_0) sample was taken. Then, hydrogen peroxide was added as the oxidizing agent, at a 41 mM concentration. At this point, the lamp was turned on and the experiment started.

Additionally to the photo-Fenton experiments, experiments with the Fenton reagent were carried out for comparison purposes. In these experiments the procedure was the same, except that the lamp was not employed.

Every experimental run lasted for 5 h. The solution was kept in agitation for the duration of the experiment and samples were taken at timed intervals, immediately quenched in NaOH solution, and analyzed. The samples taken during the photo-Fenton reaction were analyzed for H_2O_2, Fe(II), color, and total organic carbon (TOC), as described in Section 2.3, whereas those from the Fenton reagent were analyzed only for color. The rise in the reaction mixture temperature due to the heating of the solution by agitation and/or absorption of the lamp radiation by the dye was followed by a CORNING temperature meter mod. 309 (-50 to $150 \pm 0.4\,^{\circ}C$ range).

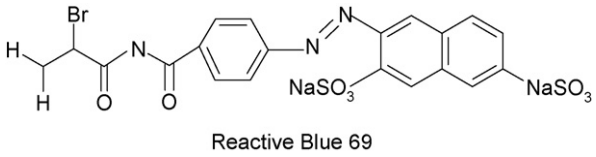

Fig. 2. Molecular structure of the reactive blue 69 azo dye.

Experiments for the RB69 azo-dye photolysis under the illumination from the lamp were also carried out. For this case, the synthetic colored solution in acidic (pH 3) conditions was placed in the reactor and the lamp was turned on for 1 h.

2.3. Analytical methods

Hydrogen peroxide concentration was determined by iodometric titration (stock solution $[H_2O_2] \geq 10^{-3}$ M). The concentration of Fe(II) was measured by the *o*-phenanthroline colorimetric method after reduction of Fe(III) with hydroxylamine chloride and by using a molar extinction coefficient of

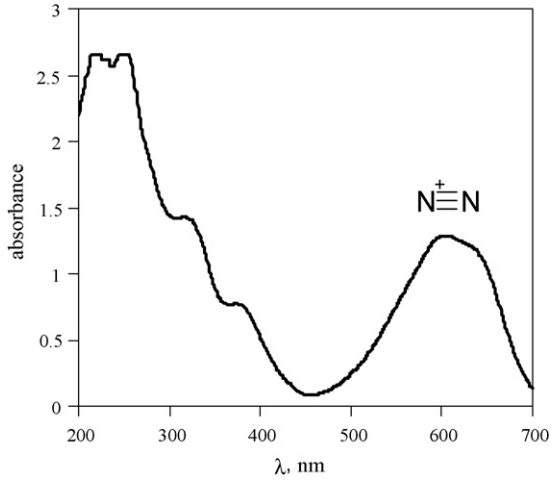

Fig. 3. UV–vis spectra for the initial concentration of the azo-dye RB69 at pH 6.8.

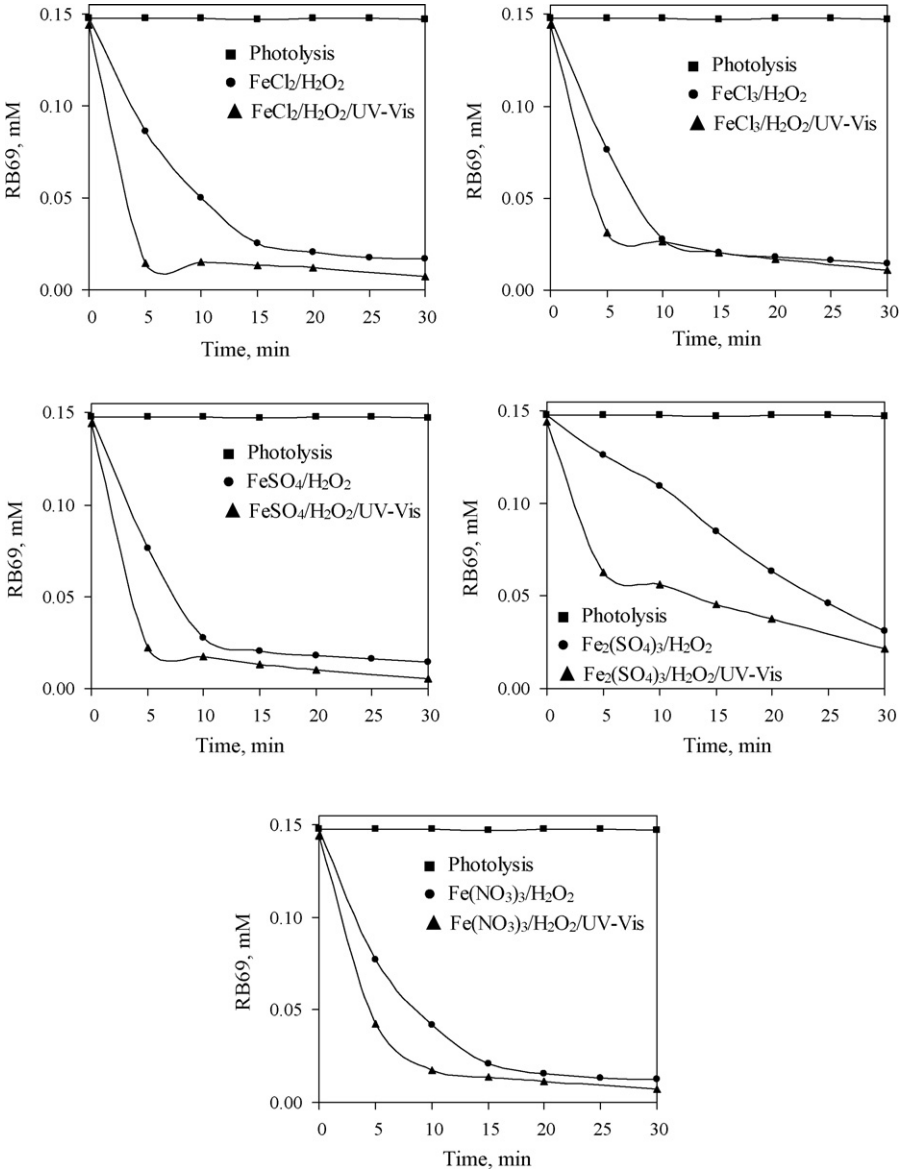

Fig. 4. Decoloration of RB69 as function of reaction time for photolysis, Fenton and photo-Fenton reaction, with different ferrous salt/H_2O_2 systems.

$1.11 \times 10^4\ M^{-1}cm^{-1}$ at 510 nm for the Fe(II)–phenanthroline complex [15].

The decrease in RB69 concentration was determined from its characteristic absorption peak at λ = 605 nm. Absorption spectra of the samples in the UV–vis were measured with a Hach DR 5000 Spectrophotometer in the wavelength range 200–700 nm, using a spectral interval of 2 nm. The pH measurements were made with an OAKTON pH meter, calibrated with standard buffers solutions of 3.00 and 7.00 ± 0.02 (25 °C) [16].

The degree of mineralization of RB69 was determined by measurements of the total organic carbon with Hach direct method for low (0.3–20 mg/L) and mid (15–150 mg/L) range TOC Testing Tube Reactor/Curvette Tubes.

3. Results and discussion

3.1. Effect of iron salt on dye decomposition

The azo-dye RB69 (molecular weight 613.13) has a several groups on its chemical structure, with different absorbance peaks in the UV–vis region. The main conjugated structures in the RB69 molecule are the azo group, the benzene and the naphthalene rings. The structure of the molecule is presented in Fig. 2. Fig. 3 shows the UV–vis absorbance spectrum of the initial azo-dye solution at pH 6.8. There are five clearly distinguishable absorption peaks: one at 605 nm, in the visible region, and four in the ultraviolet region at 370, 310, 250, and 220 nm. These absorption bands correspond to the main functional groups of the dye molecule: the chromophore group containing the azo structure produces the absorption in the visible region, while the aromatic rings absorb in the UV region. Absorbance spectra were measured at several values of pH, 1.5, 2, 2.5, 3, 4, 5, 8, 10 and no modifications were observed. This indicates that the RB69 azo-dye structure was not modified by the pH value. Also at pH 3 absorbance spectra of the dye in presence of iron ions were measured, which did not show evidence of the formation of iron–dye complexes.

In decolorization process is of special interest the evolution of the absorbance peak in the visible region (λ = 605 nm), since color in the synthetic water is related to this absorption band. In fact RB69 dye concentration is proportional to the measured absorbance at 605 nm, which is caused by the chromophore group of the molecule.

Fig. 4 shows the concentration profile of RB69 dye in photolysis (UV–vis), dark (iron/H_2O_2 systems) and photo-assisted (iron/H_2O_2/UV–vis systems) conditions. As can be observed in Fig. 4, the azo dye was not modified by the visible light. However, in dark conditions a very important decolorization of the synthetic water is observed after 10–30 min of reaction for the different salts. The most effective salts was $FeCl_3$, and the slowest, by far, was $Fe_2(SO_4)_3$.

The results of the photo-assisted process are also shown in Fig. 4. In all cases the photo-assisted process greatly increases the decolorization rate. Color diminished to very low values the first 5–10 min of reaction, with the only exception of the $Fe_2(SO_4)_3$ system. The considerable increase in the rate of decolorization observed could be attributable to the photoreduction of free ferric species which yields ferrous ion and OH radicals. It could also be attributable to the Fe(III)–peroxo (Eq. (4), Table 1) and Fe(III)–hydroperoxo complexes (Eqs. (3) and (5), Table 1), formed during reaction by interaction of H_2O_2 with Fe(III). These complexes undergo homolytic dissociation by the absorption of visible light (in the 290–550 nm wavelength range for the Fe(III)–hydroperoxo and 400–600 nm for the iron(III)–peroxo [22,23]). Nevertheless, this process is not so well known as the former.

The percentage of decolorization in dark and in photo-assisted conditions in the first 5 min of reaction is compared in Table 4. In dark conditions the percentage of decolorization is similar for the $FeCl_2$, $FeCl_3$, $FeSO_4$ and $Fe(NO_3)_3$ salts with 50% approximately of decolorization. The dye degradation with $Fe_2(SO_4)_3/H_2O_2$ system shown the smallest percentage of decolorization.

Table 4
Decolorization percent determined after 5 min of reaction, in dark and photo-assisted experimental conditions, for different iron salt/H_2O_2 systems

System	Dark	Photo-assisted
$FeCl_2/H_2O_2$	42	90
$FeCl_3/H_2O_2$	49	79
$FeSO_4/H_2O_2$	49	85
$Fe_2(SO_4)_3/H_2O_2$	15	57
$Fe(NO_3)_3/H_2O_2$	48	71

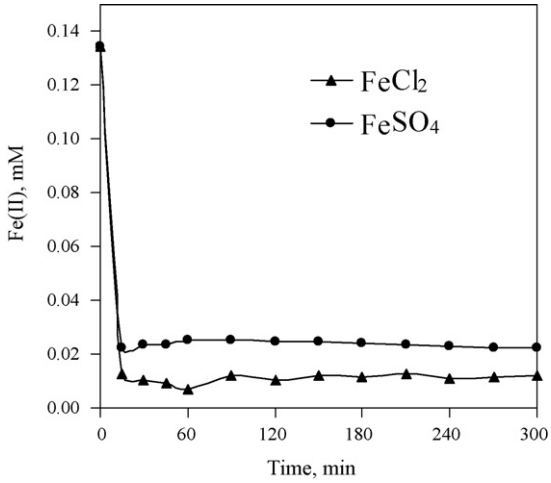

Fig. 5. Oxidation profile of Fe(II) for the different ferrous salts tested as function of reaction time.

The experimental results of the photo-assisted dye degradation are similar with previous works in the literature, in the sense that the rates of decomposition of H_2O_2 and oxidation of organic solutes are slower by Fe(III)/H_2O_2 system than by Fe(II)/H_2O_2. The salts with higher percent of decolorization were $FeCl_2$ and $FeSO_4$. This may be due to the fact that in the first minutes the rate of decomposition of hydrogen peroxide by Fe(II) (Eq. (1), Table 1) is very fast, generating high concentrations of OH• radicals, which quickly

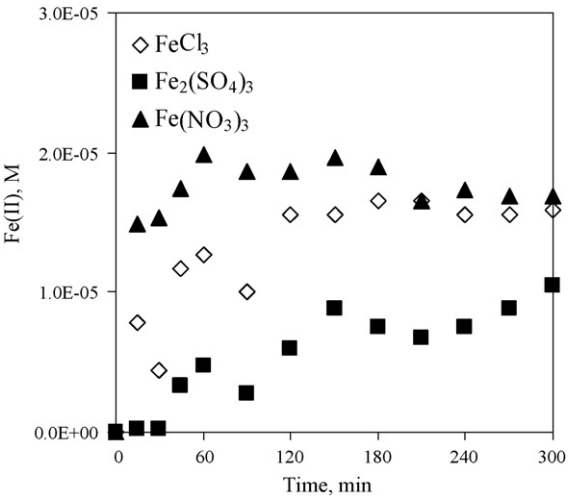

Fig. 6. Photoreduction profile of Fe(III) for the different ferric salts tested as function of reaction time.

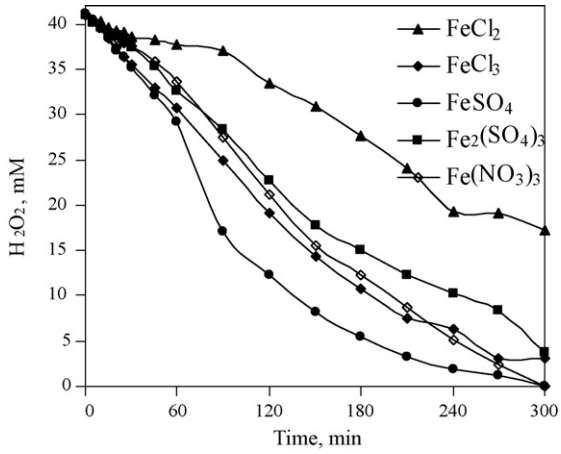

Fig. 7. Decomposition of H_2O_2 by different ferrous and ferric salts.

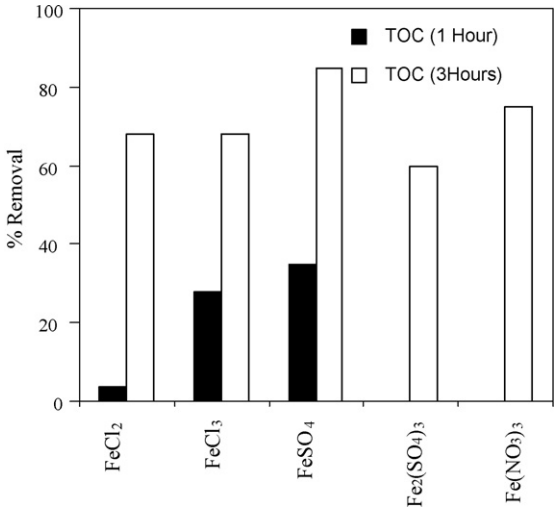

Fig. 8. TOC removal values after 1 and 3 h of reaction for the different photo-assisted systems.

oxidize the dye (Fig. 4). Actually, as can be observed in Fig. 5, the ferrous ion is completely oxidized in the first minutes of the photo-assisted reaction. In contrast, when Fe(III) salts were used (Fig. 6), some minutes of irradiation are required for the photoreduction to Fe(II).

The photo-assisted dye degradation with $Fe_2(SO_4)_3/H_2O_2$ system gave the smallest percentage of decolorization, since that oxidative species generated by rupture of Fe(III)–peroxo complexes, just like HO_2^-, are less reactive species. In this case, the decolorization process could be influenced by the effect of the sulfate anion. However, the formation Fe(III) complexes by sulfate anion (Eqs. (22)–(24), Table 3) is not very likely because of the strong competition with hydrogen peroxide (Eqs. (4) and (5), Table 1), since the sulfate anion concentration is negligible with regard to hydrogen peroxide. Thus, the photo-assisted process is only influenced by the photo-reduction of Fe(III) (Fig. 6).

We also determined the effect of the iron salt counter ion on the actual decomposition rate of H_2O_2 in photo-assisted conditions (Eqs. (1) and (4) of Table 1). These results are shown in Fig. 7.

It is interesting to note that hydrogen peroxide decomposition is effectively affected by the counter ion of ferrous chloride. The initial behavior (first 30 min) of the reaction rate has a very similar tendency for all the iron salts. This is the stage where the greatest amount of decolorization occurs, and is due to the attack from either hydroxyl radicals, for the case of Fe(II) salts, or peroxo radicals, for the case of Fe(III). In the long term, clear differences can be observed in the evolution of H_2O_2 for the different salts. While the cases of the ferric salts can be described quite well by zero order kinetics with similar rates, the ferrous salts show significant deviations from such a simple behavior.

In particular, in the case of the $FeCl_2$, the rate of decomposition of H_2O_2 shows a slower tendency in this second stage. This occurs because of the competition between H_2O_2 (Eqs. (4) and (5), Table 1) and Cl^- ions (Eqs. (11) and (12), Table 2) to form complexes with iron. In our case the concentration of Cl^- ions in solution is small (0.29 mM) in comparison with the concentration H_2O_2 (41 mM); therefore the formation of Fe(III)–chloro complexes is expected to be less important then the formation of Fe(III)–peroxo and Fe(III)–hydroperoxo complexes.

3.2. Oxidation and mineralization of the effluent

Besides color removal, oxidation and mineralization in the effluent are other bulk characterizations very useful in wastewater treatment. The actual mineralization was determined as total organic carbon. Fig. 8 shows TOC removal values after 60 and 180 min, for every iron/hydrogen peroxide system used. The initial value of TOC is 28 mg C L^{-1}.

From Fig. 8 it is noticeable that TOC values were not substantially modified during the first hour of degradation process, suggesting that, during this time, the main reaction is the azo bond breakage yielding intermediate compounds. Once the initial decolorization process slows down, the oxidizing species start reacting more with the intermediate compounds, carrying out their mineralization.

Other interesting trend can be identified when comparing TOC values obtained for the different iron salts tested: it is possible to observe in Fig. 8, that the TOC degraded is similar for ferrous and ferric salts in 3 h of reaction, where ferrous sulfate salt gives the best results with 85% degradation. These results indicate that the use of ferrous sulfate salt not only lead to chromophore group fragmentation but to mineralization of the azo-dye molecule and its intermediates. For the nitrate ferric salt a similar situation happens, with high percentages of TOC degraded in comparison with the others salts.

4. Conclusions

It was demonstrated that, as in the case of Fenton reaction, photo-assisted Fenton processes are influenced by the counter ion of the iron salt used in the reaction. For the particular case of the reactive blue 69 dye degradation, it was identified that chloride salts enhance color removal rate when compared with sulfate or nitrate salts.

The tendency observed for decoloration efficiency obtained for the different iron salts tested is not entirely in agreement with earlier reports. Nevertheless, this disagreement can actually be rationalized considering the effect of radiation field on the process: it is clear that the use of radiation will generate entirely different conditions compared with previous works, mainly by photoreduction of Fe(III), leading to novel degradation pathways still to be studied.

If color removal is considered as the main parameter to be considered for textile wastewater reuse, results provided by this work are very interesting because color was almost completely removed in about 10 min, when ferrous chloride salt was used. Use of other ferrous and ferric salts (except ferric sulfate) provides similar trends with almost equivalent initial reaction rates. When mineralization is considered as the actual goal of the process, it was determined

that sulfate salts (specifically ferrous sulfate) are the most appropriate to be used in the reaction mixture.

Acknowledgements

The authors gratefully acknowledge to PAPIIT for the financial support of this project (grant IN215606) and to Rogelio Morán Elvira for his technical support.

References

[1] V.M. Correia, T. Stephenson, S.J. Judd, Characterization of textile wastewaters: a review, Environmental Technology 15 (1994) 917–929.
[2] E.R. Bandala, M.A. Pelaez, A.J. García, M.J. Salgado, G. Moeller, Photocatalytic decolorization of synthetic and real textile wastewater containing benzidine-based azo dyes, Chemical Engineering and Processing 47 (2008) 169–176.
[3] E.N. Leshem, D.S. Pines, S.J. Ergas, D.A. Rechow, Electrochemical oxidation and oxidation for textile wastewater reuse, Journal of Environmental Engineering 132 (2006) 324–330.
[4] P.C. Vandevivere, R. Bianchi, W. Verstraete, Treatment and reuse of wastewater from the textile wet-processing industry: review of emerging technologies, Journal of Chemical Technology and Biotechnology 72 (1998) 289–302.
[5] S.J. Ergas, D.M. Therriault, D.A. Reckhow, Evaluation of water reuse technologies for the textile industry, Journal of Environmental Engineering 132 (2006) 315–323.
[6] I. Arslan, I.A. Bacioglu, T. Tuhkanen, Advanced oxidation of synthetic dyehouse effluent by O_3, O_3/H_2O_2 and H_2O_2/UV processes, Environmental Technology 20 (1999) 921–931.
[7] S. Kang, C. Liao, S. Po, Decoloration of textile wastewater by photo-Fenton oxidation technology, Chemosphere 41 (2000) 1287–1294.
[8] W. Feng, D. Nansheng, H. Heling, Degradation mechanism of azo dyes C.I. reactive red by iron powder reduction and photooxidation in aqueous solutions, Chemosphere 41 (2000) 1233–1238.
[9] J. Kiwi, O. Enea, Photo-assisted Fenton degradation of model textile dyes by Fe/Nafion/glass fibers under solar radiation, in: Proceedings of the 11th SolarPACES Conference, September 4–6, Zurich, Switzerland, 2002.
[10] J.M. Chacon, M.T. Leal, M. Sanchez, E.R. Bandala, Solar photocatalytic degradation of azo-dyes by photo-Fenton process, Dyes and Pigments 69 (2006) 144–150.
[11] A.Y. Sychev, V.G. Issak, Iron compounds and the mechanism of the homogeneous catalysis of the activation of O_2 and H_2O_2 and the oxidation of organic substrates, Russian Chemical Reviews 64 (1995) 1105–1129.
[12] J. De Laat, G. Le Troung, B. Legube, A comparative study of the effects of chloride sulfate and nitrate ions on the rates of decomposition of H_2O_2 and organic compounds by Fe(II)/H_2O_2 and Fe(III)/H_2O_2, Chemosphere 55 (2004) 715–723.
[13] J. De Laat, T.G. Le, Effects of chloride ions on the iron (III)-catalyzed decomposition of hydrogen peroxide and on the efficiency of the Fenton-like oxidation process, Applied Catalysis B: Environmental 66 (2006) 137–146.
[14] J. Kiwi, A. Lopez, V. Nadtochenko, Mechanism and kinetics of the HO-radical intervention during Fenton oxidation in the presence of a significant amount of radical scavenger (Cl^-), Environmental Science and Technology 34 (2000) 2162–2168.
[15] H. Tamura, K. Goto, T. Yotsuyanagi, M. Nagayama, Spectrophotometric determination of iron (II) with 1,10-phenantrholine in the presence of large amounts of iron (III), Talanta 21 (1974) 314–318.
[16] Standard Methods for the Examination of Water and Wastewater, 18th Edition, American Public Health Association (APHA), United States of America, 1992.
[17] J.J. Pignatello, D. Liu, P. Houston, Evidence for an additional oxidant in the photoassisted Fenton reaction, Environmental Science and Technology 33 (1999) 1832–1839.
[18] G.L. Truong, J. De Laat, B. Legube, Effects of chloride and sulfate on the rate of oxidation of ferrous ion by H_2O_2, Water Research 38 (2004) 2383–2393.
[19] H.A. Schwarz, R.W. Dodson, Equilibrium between hydroxyl radicals and thallium (II) and the oxidation potential of HO(aq), Journal of Physical Chemistry 88 (1984) 3643–3647.
[21] F. Haber, J. Weiss, The catalytic decomposition of hydrogen peroxide by iron salts, Proceedings of the Royal Society A 134 (1934) 332–351.
[22] H. Gallard, J. De Laat, B. Legube, Spectrophotometric study of the formation of iron (III)–hydroperoxy complexes in homogeneous aqueous solutions, Water Research 33 (1999) 2929–2936.
[23] H. Gallard, J. De Laat, Kinetic modeling of Fe(III)/H_2O_2 oxidation reactions in dilute aqueous solutions using atrazine as a model organic compounds, Water Research 34 (2000) 3107–3116.
[24] V. Nadtochenko, J. Kiwi, Primary photochemical reactions in photo-Fenton system with ferric chloride. A case study of xylidine oxidation as a model compound, Environmental Science and Technology 32 (1998) 3273–3281.